Heterogeneous Photocatalysis, Part XIX

Semiconductor Type A Photocatalysis: Role of Substrate Adsorption and the Nature of Photoreactive Surface Sites in Zinc Sulfide Catalyzed C–C Coupling Reactions[±]

Gerald Hörner,[a] Petra Johne,[a] Ronald Künneth,[a] Günther Twardzik,[a] Henryette Roth,[b] Timothy Clark,[b] and Horst Kisch*[a]

Abstract: The mechanism of the photodehydrodimerization of 2,5-dihydrofuran (2,5-DHF) by suspended zinc sulfide powders was investigated through emission, inhibition, adsorption, and quantum yield studies. Zinc and cadmium ions influenced the emission intensity only marginally but strongly inhibited the reaction, so the photoreactive surface sites were not identical with the emitting states, which had lifetimes in the 0.1–24 ns range. Adsorption isotherms for these metal ions and 2,5-DHF in aqueous solution indicated the presence of mono- and multilayer adsorption. Zn^{2+} and Cd^{2+} were both adsorbed physically and by metal sulfide precipitatation, but in the case of Cd^{2+} a lattice exchange mechanism with ZnS afforded CdS and dissolved zinc ions also. ^{13}C NMR spectra and the good agreement between the calculated number of zinc sites and the measured amount of 2,5-DHF in the saturated solvent–solute surface monolayer indicated that 2,5-DHF was adsorbed perpendicular to the surface at all the available zinc sites. The true adsorption constant ($170 \pm 30\ L\,mol^{-1}$) was consistent with the pseudo-constant ($260 \pm 50\ L\,mol^{-1}$) obtained from the concentration dependence of the reaction rate. ^{13}C NMR signals of the α-carbon atoms of 2,5-DHF and THF adsorbed onto ZnS from the gas phase were downfield shifted by 1.5 and 0.7 ppm as compared to those of the free substrates, respectively. The downfield shift of the olefinic signals was about 0.4 ppm. It is postulated that a dissociative electron transfer from adsorbed 2,5-DHF to the reactive hole afforded a proton and the dihydrofuryl radical. The corresponding C–H bond dissociation energies were calculated by ab initio methods for various substrates. As expected, the apparent quantum yield of various substrates increased linearly with decreasing C–H bond dissociation energy. The intermediate dihydrofuryl radical dimerized to the products in the adsorbed state, as indicated by the linear increase of the square root of the reaction rate with increasing 2,5-DHF surface concentration and by competition experiments with THF/2,5-DHF mixtures. The reaction inhibition by Zn^{2+} and Cd^{2+} could be analyzed in terms of the Stern–Volmer model only when the *surface concentration* was considered. Inhibition by Cd^{2+} is about three times faster than inhibition by Zn^{2+}, in which case no zinc metal was observed.

Keywords: ab initio calculations · C–C coupling · photochemistry · surface chemistry · zinc sulfide

Introduction

The mechanism of semiconductor-catalyzed photoreactions has been investigated quite thoroughly for colloidal systems[1] since their pseudo-homogeneous nature allows application of spectroscopic methods in situ. This is not true—except for a few diffuse reflectance studies[2]—for powder suspensions, although these are more important for chemical synthesis.[3] In both systems, however, two basic mechanistic questions could not be answered. Firstly, only a very few studies have dealt with the problem of whether emissive (e^-_{tr}, h^+_{tr}) and reactive (e^-_r, h^+_r) surface sites are identical; it has been observed, for example, that substrates such as $NHEt_2$ which are photooxidized on ZnS powders do not affect the static emission spectra.[4] Secondly, there is only scarce experimental evidence on whether the primary redox intermediates are transformed to the final products in an adsorbed or in a fully solvated state; a typical example is the CdS-catalyzed photodimerization of *N*-vinylcarbazole. From the influence of different substrate concentrations on reaction rate it was proposed that the intermediate radical cation reacts with both adsorbed and solvated *N*-vinylcarbazole.[5] However, the interpretation of such experiments is not straightforward[6]

[a] Prof. Dr. H. Kisch, Dipl.-Chem. G. Hörner, Dr. P. Johne, Dr. R. Künneth, Dr. G. Twardzik
Institut für Anorganische Chemie der Universität Erlangen-Nürnberg
Egerlandstrasse 1, D-91058 Erlangen (Germany)
Fax: (49) 9131 8527363
E-mail: kisch@anorganik.chemie.uni-erlangen.de

[b] Dipl.-Chem. H. Roth, Dr. T. Clark
Institut für Organische Chemie der Universität Erlangen-Nürnberg
Nägelsbachstrasse 25, D-91054 Erlangen (Germany)

[±] Part XVIII: H. Kisch, L. Zang, C. Lange, W. F. Maier, C. Antonius, D. Meissner, *Angew. Chem.* **1998**, *110*, 3201; *Angew. Chem. Int. Ed.* **1998**, *37*, 3034.

0947-6539/99/0501-0208 $ 17.50+.50/0

and the pseudo-adsorption constant obtained from a plot of reciprocal rate against reciprocal initial substrate concentration may differ significantly from the true constant measured directly, as was reported for the adsorption of alcohols and imines onto TiO_2 and CdS, respectively.[7] Here we try to answer these two questions for the ZnS catalyzed photodehydrodimerization of 2,5-dihydrofuran (2,5-DHF), a rare example of a new compound being obtained by semiconductor photocatalysis on a preparative scale.[8] The reaction can be classified as type A semiconductor photocatalysis since both a reduction and an oxidation product are obtained.[3d] It was assumed that the photogenerated electron–hole pair reduces water to hydrogen and OH^-, and oxidizes the ether to the dihydrofuryl radical and H^+. Dimerization of the former affords a statistical mixture of regioisomeric dehydrodimers [Eq. (1)], which could be separated by preparative gas chromatography. Quantitative measurements revealed a stoichiometric ratio of 1:1 for the dehydrodimers and hydrogen.[8b]

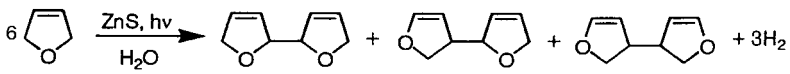

(1)

However, it could not be decided whether emitting and reactive electron–hole pairs are identical—as was also the case in the recent EPR spectroscopic observation of different types of trapped holes and electrons on irradiated ZnS particles[9]—and whether radical C–C coupling occurs at the surface or in solution. In order to answer these two basic questions for this reaction, we investigated the effect of electron scavengers on the emission and photocatalytic activity of various ZnS powders, the influence of substrate concentration on reaction rate, the nature of substrate adsorption, and the variation of apparent product quantum yield with the oxidation potential and the corresponding C–H bond dissociation energy of various substrates. Recently Yanagida et al. reported on similar photodehydrodimerizations catalyzed by ZnS nanocrystallites.[10] The chemoselectivity of this photocatalyst is different from that of the large particles (≥ 0.2 μm) employed in our studies; for example, dioxane is dehydrodimerized by the former but not by the latter catalyst system.

Abstract in German: *Der Mechanismus der unter Wasserstoffentwicklung verlaufenden Zinksulfid-katalysierten Photodehydrodimerisierung von 2,5-Dihydrofuran (2,5-DHF) wurde durch Emissions-, Adsorptions- und Inhibierungsexperimente sowie Quantenausbeutebestimmungen untersucht. Da Zink- und Cadmiumionen die Emission nur geringfügig beeinflussen, die Reaktion aber inhibieren, sind die photoreaktiven Oberflächenzustände mit den emittierenden ($\tau = 0.1-24$ ns) nicht identisch. Adsorptionsisothermen dieser Metallionen sowie von 2,5-DHF deuten auf Mono- und Multischichtadsorption. Während Zn^{2+} und Cd^{2+} sowohl physisorbieren als auch in Form des Metallsulfids gefällt werden, wird im Falle von Cd^{2+} eine teilweise Umfällung zu CdS und gelösten Zinkionen beobachtet. ^{13}C NMR Spektren und der Vergleich der für kubisches ZnS theoretisch verfügbaren Anzahl von Zinkzentren mit dem Belegungsgrad in der gesättigten Wasser-2,5-DHF-Monoschicht deuten darauf hin, daß 2,5-DHF senkrecht zur Oberfläche über das Sauerstoffatom adsorbiert ist. Die wahre Adsorptionskonstante von 170 ± 30 L mol^{-1} entspricht der aus der Konzentrationsabhängigkeit der Reaktionsgeschwindigkeit erhaltenen scheinbaren Konstante von 260 ± 50 L mol^{-1}. Werden 2,5-DHF und THF aus der Gasphase auf ZnS adsorbiert, verschieben sich die ^{13}C NMR-Signale der α-Kohlenstoffatome im Vergleich zur homogenen Lösung um 1.5 bzw. 0.7 ppm zu tieferem Feld, diejenigen der olefinischen Kohlenstoffatome dagegen nur um 0.4 ppm. Es wird angenommen, daß 2,5-DHF von einem Defektelektron unter gleichzeitiger Deprotonierung zum Dihydrofurylradikal und einem Proton oxidiert wird. Die mittels ab initio Methoden berechneten C-H - Bindungsdissoziationsenergien korrelieren mit den scheinbaren Quantenausbeuten. Konkurrenzexperimente mit 2,5-DHF/THF und die lineare Abhängigkeit der radizierten Reaktionsgeschwindigkeit von der Oberflächenkonzentration an 2,5-DHF deuten auf eine Dimerisierung der intermediären Dihydrofurylradikale im adsorbierten Zustand. Nur bei Verwendung der Oberflächenkonzentrationen von Cd^2 und Zn^{2+} läßt sich die Inhibierung im Rahmen des Stern-Volmer Modells quantitativ auswerten. Danach reagiert Cd^{2+} dreimal schneller als Zn^{2+} und wird zu Cd^0 reduziert, wohingegen im letzteren Falle kein elementares Zink entsteht.*

Results

Emission and activity studies: From previous work it was known that precipitation of ZnS from aqueous $ZnSO_4$ solutions by addition of Na_2S or thiourea gave ZnS-A and ZnS-B type powders as the most active photocatalysts.[11] To vary the zinc/sulfur ratio of type A samples, precipitation was also performed in the presence of a 20 mol % excess of S^{2-} (ZnS-A/S^{2-}) and Zn^{2+} (ZnS-A/Zn^{2+}). For type B powders, the hydrolysis times of 48 and 1 h afforded slightly pink ZnS-B_1 and white ZnS-B_2, respectively.

The initial reaction rates depend strongly on the preparation conditions (Table 1). The activity of both ZnS-A and ZnS-A/S^{2-} reaches 85 % of that of ZnS-B_1, the most reactive sample (85 mL h^{-1}), indicating that additional sulfide has a negligible effect on the already sulfur-rich powder.[11] Correspondingly, the activity of neither ZnS-B_1 nor ZnS-A is affected by the presence of sulfide ions at concentrations of $c_s \leq 0.7$ mol g^{-1}.[12] ZnS-B_2 still has 16 % of the ZnS-B_1 activity, but ZnS-A/Zn^{2+} is almost inactive. This is in accord with the action of zinc ions as recombination centers for electron–hole pairs.[13] Addition of $ZnSO_4$ and $CdSO_4$ resulted in a moderate and strong inhibition, respectively. No hydrogen evolution was detected with the commercial ZnS–Ventron (purity > 99.99 %) and a ZnS colloid, prepared according to reference [14]. All samples were photostable except ZnS–Ventron

Table 1. Dependence of intensity (I) of SA emission at 430 nm and initial reaction rate ($v(H_2)$) in the absence (v°, I°) and presence (v, I) of zinc and cadmium ions.

Sample	Additive	c_s [mmol g^{-1}]	$v^\circ(H_2)/v(H_2)$	I°/I
ZnS-A	–	–	1.0[a]	1.0[c]
	Zn^{2+}	0.44	1.3	0.8
	Zn^{2+}	44.5	3.0	1.3
	Cd^{2+}	0.44	16	1.7
	Cd^{2+}	44.5	∞	2.0
ZnS-A/Zn^{2+}	–	–	42.5	0.8
ZnS-A/S^{2-}	–	–	1.0	9.0
ZnS-B_1	–	–	1.0[b]	1.0[c]
	Zn^{2+}	0.44	2.6	0.8
	Zn^{2+}	44.5	6.0	1.3
	Cd^{2+}	0.44	13	1.0
	Cd^{2+}	44.5	∞	1.0
ZnS-B_2	–	–	6	0.5
ZnS-Ventron	–	–	∞	0.5

[a] ZnS-A: $v^\circ(H_2) = 72$ mL h^{-1}. [b] ZnS-B_1: $v^\circ(H_2) = 85$ mL h^{-1}. [c] The ratio of SA intensities of ZnS-A to ZnS-B_1 is 8:1.

and ZnS-B_2, which photocorroded to sulfur and elemental zinc in either the presence or absence of 2,5-DHF.

The emission spectra ($\lambda_{exc} = 320$ nm) of aqueous suspensions of ZnS-A and ZnS-B_1 are summarized in Figure 1.

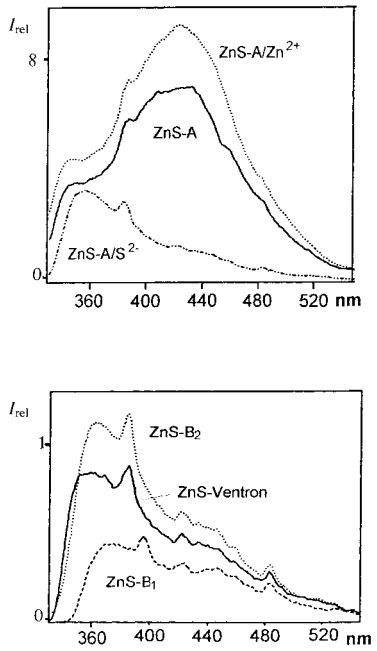

Figure 1. Emission spectra of various aqueous ZnS powder suspensions (0.02 g in 3.5 mL of H_2O, $\lambda_{exc} = 320$ nm). I_{rel} = relative intensity in arbitrary units.

Mutual contributions from colloidal zinc sulfide can be excluded since no emission could be detected from a solution obtained by filtration of the suspension through a micropore filter (pore size = 0.2 μm). For ZnS-A and ZnS/Zn^{2+}, in agreement with the literature,[13] the self-activated (SA) emission at 430 nm due to zinc centers (that is, sulfur vacancies) is more intense than the band-gap emission (Figure 1, upper panel), while the opposite is observed for ZnS – Ventron, for the type B powders, for ZnS-A/S^{2-} (Figure 1, lower panel), and for ZnS-A in the presence of sodium sulfide (0.16 mol g^{-1}, not shown). The latter results suggest that the added sulfide ions block the zinc centers involved in the SA emission. Correspondingly, the emission spectrum of ZnS-B_1, which shows only a very weak SA band, is not changed upon addition of sodium sulfide. Addition of $ZnSO_4$ (4.4×10^{-4} mol g^{-1}) to a suspension of ZnS-A or ZnS-B_1 increased both the SA and band-gap emissions by 25%, whereas a decrease of 25% occurred at the 100-fold (4.4×10^{-2} mol g^{-1}) zinc concentration (Table 1). In contrast, addition of $CdSO_4$ to ZnS-A decreased the SA emission by 40%, already at the lower concentration, and no effect was observable in the case of ZnS-B_1, even at the higher concentration.

Time-resolved emission spectra ($\lambda_{exc} = 306$ nm) of ZnS-A and the inactive ZnS – Ventron revealed multiexponential decay at all three emission wavelengths investigated (340, 389, and 437 nm). Curve fitting for the last two afforded best results with a four- and three-component system for ZnS-A and ZnS – Ventron, respectively. The corresponding calculated lifetimes were all in the 0.1 – 24 ns range. The longest lifetimes were 12 (ZnS – Ventron) and 24 ns (ZnS-A), values also found for ZnS colloids[15] and powders.[16] As noted in the literature, apparent multiexponential behavior may arise not only from different emitting states but also from a distribution in particle size.[17] Addition of 2,5-DHF had no significant effect on lifetimes.

Adsorption experiments: In dark adsorption experiments, aqueous suspensions of ZnS-B_1 with $CdSO_4$ and $ZnSO_4$ were stirred overnight at ambient temperature, then the residual concentrations of dissolved Cd^{2+} and Zn^{2+} ions were measured and n_{eq}, the molar amount of metal ions adsorbed per gram of ZnS, was calculated. Both the ions behave similarly up to a concentration c_s of 0.8×10^{-4} mol g^{-1} (Figure 2), above

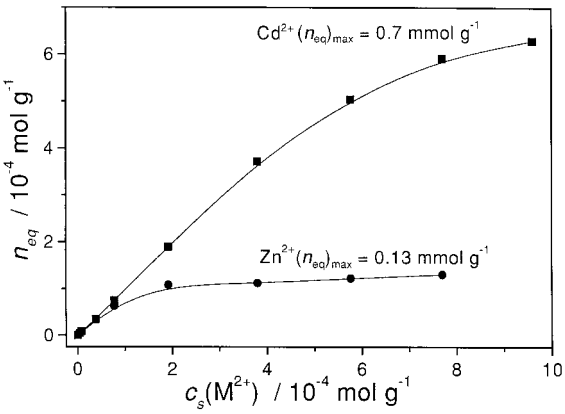

Figure 2. Adsorption of $ZnSO_4$ and $CdSO_4$ onto ZnS-B_1 (1.3 g L^{-1}).

which the zinc isotherm reaches a saturation plateau at $n_{eq} = 1.3 \times 10^{-4}$ mol g^{-1}; a second adsorption step follows, with a coverage about 15 times higher (not shown) at concentrations above 3×10^{-3} mol g^{-1},[18] similarly to the adsorption of Ag^+ onto TiO_2.[19] In the case of cadmium the linear increase develops into a plateau at a coverage of about 7×10^{-4} mol g^{-1}. Analysis of the adsorption data in terms of the

0947-6539/99/0501-0210 $ 17.50+.50/0 *Chem. Eur. J.* **1999**, *5*, No. 1

Hiemenz model (vide infra) is not possible, because the adsorption equilibrium is too complicated.[20]

To obtain the adsorption constant of 2,5-DHF, the amount adsorbed onto ZnS-B_1 was determined as described above for the metal ions. A plot of the equilibrium coverage against residual substrate concentration (Figure 3) exhibits two

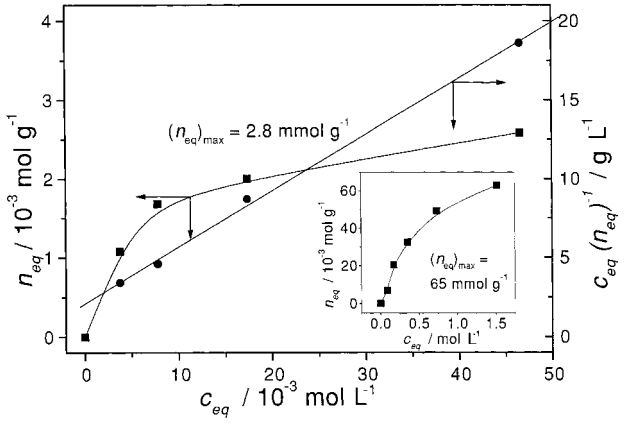

Figure 3. Adsorption of 2,5-DHF onto ZnS-B_1 (1.3 g L^{-1}) (inset: total concentration range) (■) and Hiemenz linearization plot (●).

saturation plateaus at $(n_{eq})_{max} = 2.8 \times 10^{-3}$ and 65×10^{-3} mol g^{-1}. This indicates multilayer adsorption as commonly observed in heterogeneous catalysis.[21] The first adsorption plateau is therefore attributed to a filled surface monolayer.

The adsorption data were analyzed by application of the Hiemenz model,[22] as recently reported for photoreactions catalyzed by TiO_2[7a] or CdS.[7b] In those cases the formation of an ideal mixed solvent–solute surface monolayer according to Equation (2) (where the superscripts b and s indicate bulk solution and surface layer, respectively) is assumed.

$$H_2O^s + 2{,}5\text{-DHF}^b \rightleftharpoons H_2O^b + 2{,}5\text{-DHF}^s \quad (2)$$

Hiemenz arrived at Equation (3), where K_{ad} is the equilibrium constant divided by the bulk water concentration, σ° the average area occupied by the molecule in the saturated solvent–solute surface monolayer, A_{sp} the specific surface area of ZnS-B_1 (170 m^2 g^{-1}) and N_A the Avogadro number.

$$\frac{c_{eq}}{n_{eq}} = \frac{N_A \sigma^o}{A_{sp} K_{ad}} + \frac{N_A \sigma^o}{A_{sp}} c_{eq} \quad (3)$$

A plot of $c_{eq}(n_{eq})^{-1}$ against c_{eq} exhibits good linearity (Figure 3; least-squares regression coefficient = 0.999). From slope and intercept (slope = 3.56×10^2 g mol^{-1}; intercept = 2.09 g L^{-1}) values of 170 ± 30 L mol^{-1} and 10.2 Å^2 are calculated for the adsorption constant K_{ad} and the area occupied by 2,5-DHF, respectively.

Concentration dependence: The dependence of the reaction rates on the initial concentrations of THF and 2,5-DHF was measured (Figure 4). The maximum rate of hydrogen evolution for THF was found to be only 10% of that for 2,5-DHF. A concentration of 5 mol g^{-1} of THF is required to obtain the maximum rate, whereas only 0.4 mol g^{-1} is necessary for 2,5-

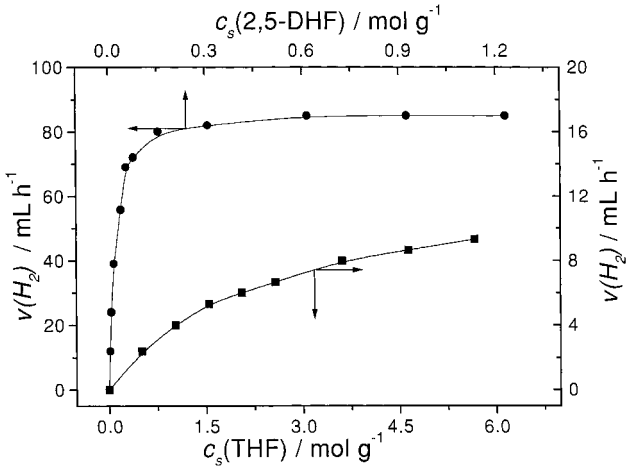

Figure 4. Dependence of initial hydrogen evolution rate on 2,5-DHF (●) and THF (■) concentrations.

DHF. In contrast to the related CdS-catalyzed addition of 2,5-DHF to azobenzenes and Schiff bases,[7b] no induction period was observed.

Inhibition by Zn^{2+} and Cd^{2+}: A Stern–Volmer plot of the dependence of the reaction rate on the concentration of added $ZnSO_4$ and $CdSO_4$ is depicted in Figure 5 for ZnS-B_1. Half-inhibition is found for Zn^{2+} and Cd^{2+} at $c_s = 1.80 \times 10^{-4}$ and 0.20×10^{-4} mol g^{-1}, respectively. In the case of Zn^{2+} a plateau at about 0.6×10^{-3} mol g^{-1} is followed by a further

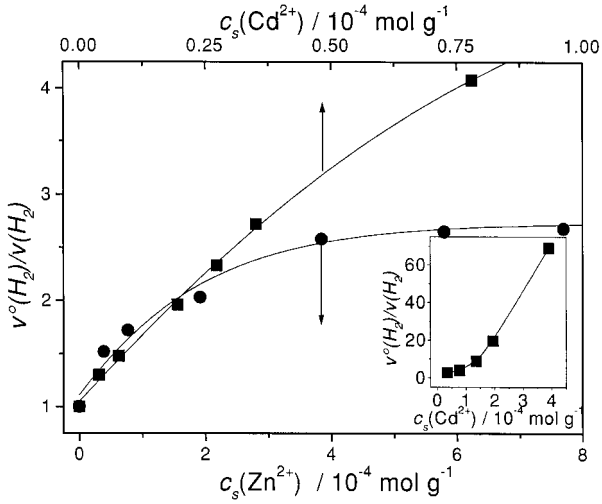

Figure 5. Stern–Volmer plots of reaction inhibition by dissolved Cd^{2+} and Zn^{2+} ions.

increase and a second plateau at concentrations higher than 2×10^{-2} mol g^{-1} (not shown). For Cd^{2+}, after an almost linear increase of $v^\circ(H_2)/v(H_2)$ up to 0.5×10^{-4} mol g^{-1} there is an exponential increase (see Figure 5, inset), leading to total inhibition at $c_s = 6 \times 10^{-4}$ mol g^{-1} (not shown in Figure 5). Even at a concentration of only 3.9×10^{-6} mol g^{-1} this is accompanied by the formation of elemental cadmium, as evidenced by the reduction of added MV^{2+} to the blue radical cation $MV^{\bullet+}$. When a 465 nm cut-off filter was employed to

exclude ZnS excitation, no Cd^0 was produced; thus photocorrosion through excitation of surface-formed CdS can be ruled out. In the case of Zn^{2+} neither darkening of the catalyst nor total inhibition—even at a zinc ion concentration of $c_s = 0.8\ mol\,g^{-1}$—could be detected.

Discussion

Adsorption of Zn^{2+} and Cd^{2+} on the ZnS-B_1 surface: For the adsorption of a metal ion ($M^{2+}_{(l)}$) onto a hydrous metal sulfide surface, generally three mechanisms are discussed: i) Precipitation as $M_{(l)}S$; ii) lattice exchange, $MS_{(s)} + M^{2+}_{(l)}) = M_{(l)}S_{(s)} + M^{2+}$; and iii) adsorption, $MS_{(s)} + M^{2+}_{(l)} = MS_{(s)} - M^{2+}_{(l)}$.[23] For Zn^{2+} adsorption only mechanisms i and iii can be considered, but because CdS has a much lower solubility product ($L = 2 \times 10^{-28}\ mol^2\,L^{-2}$) than ZnS ($L = 4 \times 10^{-24}\ mol^2\,L^{-2}$), mechanism ii is also expected to operate for Cd^{2+} ions. The lattice exchange mechanism (ii) was also proposed in studies concerned with emission quenching on colloidal zinc sulfide by Ren and co-workers, although no CdS could be detected.[24] Our results were different, and in accordance with those of Henglein and co-workers:[25] a weak peak at 520 nm in the excitation spectrum ($\lambda_{em} = 540$ nm) suggests the presence of CdS. More direct support was obtained by monitoring the concentration of zinc ions in the solution upon addition of cadmium sulfate. The relationship between the concentration of desorbed zinc ions (c_s) and the coverage of adsorbed cadmium ions (n_{eq}) reveals that c_s increases significantly only after n_{eq} reaches a threshold of $0.8 \times 10^{-4}\ mol\,g^{-1}$ (Figure 6).

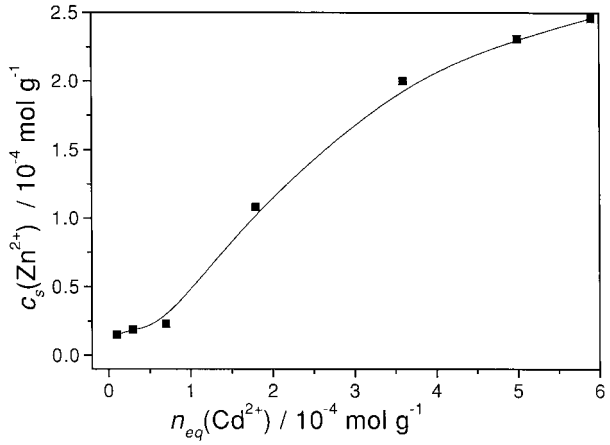

Figure 6. Dependence of Zn^{2+} ion desorption on Cd^{2+} ion adsorption.

This agrees well with the concentration up to which zinc and cadmium ions exhibit similar adsorption behavior (see Figure 2), most probably by precipitation and adsorption mechanisms. Since the maximum slope of the $c_s - n_{eq}$ plot is only about 0.6 (Figure 6), the difference from 1.0 suggests that even above the threshold the two other mechanisms are still important. Detailed studies indicate that mechanism iii can be described as substitution of a proton in a surface [Zn]–OH or [Zn]–SH group by Cd^{2+} or Zn^{2+}.[20]

Effect of Zn^{2+} and Cd^{2+} on SA emission and reactivity: The weak increase in intensity of both ZnS-A and ZnS-B_1 emissions at a low zinc concentration ($4.4 \times 10^{-4}\ mol\,g^{-1}$), which corresponds to near-saturation of the first adsorption step (Figure 2), is most probably due to an increase of the number of surface zinc centers responsible for the SA emission. At the higher concentration, $4.4 \times 10^{-2}\ mol\,g^{-1}$, the additional ions are adsorbed in a solvent–solute multilayer and function as recombination centers, resulting in a decrease in intensity. This can be rationalized as a double electron transfer quenching [Eqs. (4), (5)]. In agreement with this

$$e^-_{tr} + M^{2+} \rightarrow M^+ \quad (4)$$

$$h^+_{tr} + M^+ \rightarrow M^{2+} \quad (5)$$

explanation, Mg^{2+} and Al^{3+} ions, which are more difficult to reduce, have no significant effect on either the emission spectrum or the activity of ZnS-A. In contrast to Zn^{2+}, Cd^{2+} reduces the SA emission of ZnS-A even at the lower concentrations of the monolayer regime. This stronger effect may be due to a faster quenching by electron transfer ($E^\circ_{(Cd^{2+}/Cd)} = -0.40$ V, $E^\circ_{(Zn^{2+}/Zn)} = -0.78$ V)[26] and the formation of surface CdS.

Although the presence of S^{2-} ($0.7\ mol\,g^{-1}$) causes 90% quenching of emission it does not affect the initial rate induced by ZnS-A, which also remains unchanged when ZnS-A/S^{2-} is employed. The changes in SA emission and reactivity (Table 1) induced by the two metal ions also reveal opposite trends. This indicates that emitting (e^-_{tr}, h^+_{tr}) and reactive (e^-_r, h^+_r) states are different (Scheme 1). The same argument holds for the band-gap emission. In agreement with this conclusion, 2,5-DHF does not influence the emission spectra, even at the very high concentration ($0.7\ mol\,g^{-1}$) at which surface saturation occurs.

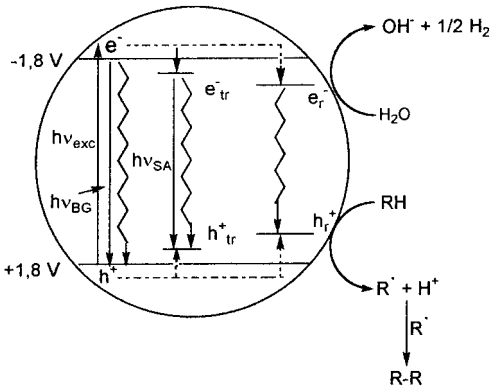

Scheme 1. Simplified mechanism; the potentials of the valence and conduction band edges apply to a ZnS single crystal at pH 7;[36d] values for the reactive e^-_r/h^+_r pair are tentative.

In the case of ZnS-B_1, which has a larger surface excess of sulfur than ZnS-A_1,[11] addition of sulfide ions leaves both emission and reactivity unchanged. However, since cadmium ions do not influence the emission but strongly inhibit the reaction (Table 1), for ZnS-B_1 also the emitting and reacting

0947-6539/99/0501-0212 $ 17.50+.50/0 *Chem. Eur. J.* **1999**, *5*, No. 1

states are different. The dependence of the reduced reaction rate on the inhibitor concentration is in agreement with these findings (Figure 5). Half-inhibition is observed even at low concentrations of *dissolved* metal ions (0.20×10^{-4} for Cd^{2+} and 1.80×10^{-4} mol g^{-1} for Zn^{2+}) at which the SA emission is either unaffected or even more intense than in the absence of the ions. The linear dependence of the reduced rate on the concentration of metal ions *adsorbed* (Figure 7) within the

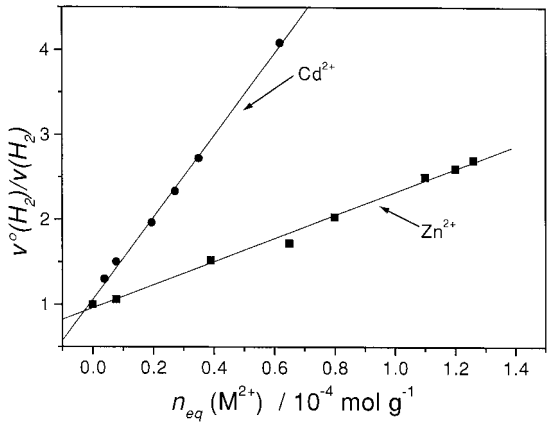

Figure 7. Stern–Volmer plots of reaction inhibition by adsorbed Cd^{2+} and Zn^{2+} ions.

solvent–solute monolayer suggests that quenching can be described by the Stern–Volmer model.[27] From the corresponding slopes, Stern–Volmer constants (k_{sv}) of 50×10^3 L mol^{-1} and 13×10^3 L mol^{-1} are calculated for Cd^{2+} and Zn^{2+} ions, respectively.[28] Since no elemental zinc is produced in the inhibition process, the zinc ions may prevent formation of the photoreactive electron–hole pair (see Scheme 1) and/or enable its efficient radiationless recombination through double electron transfer analogous to Equations (4), (5). The first alternative is more likely, since at this concentration Zn^{2+} ions increase the SA emission. In contrast, Cd^{2+} ions do not influence the emission but afford elemental cadmium during irradiation. Under conditions of total inhibition of hydrogen evolution, small amounts of the dehydrodimers but no furan could be detected as oxidation products, suggesting for the first time a decoupling of substrate oxidation and water reduction.

ZnS-B_1 photocatalysis

Dependence of reaction rate on the concentration of adsorbed 2,5-DHF: The similarity in the dependence of rate and amount of 2,5-DHF adsorbed (n_{eq}) on the concentration strongly corroborates the dominant role of substrate adsorption (Figure 8). Further support stems from the quadratic dependence of initial rate on n_{eq}, which can be linearized (Figure 9). This corresponds to the well-known case of heterogeneous catalytic dimerization by a modified Langmuir–Hinshelwood mechanism affording easily desorbable products.[29] It suggests that the dimerization of the intermediate dihydrofuryl radicals is involved in the rate-determining step and that—at least for early reaction stages—the concentration of these adsorbed radicals increases linearly with n_{eq}, the surface concentration of 2,5-DHF.

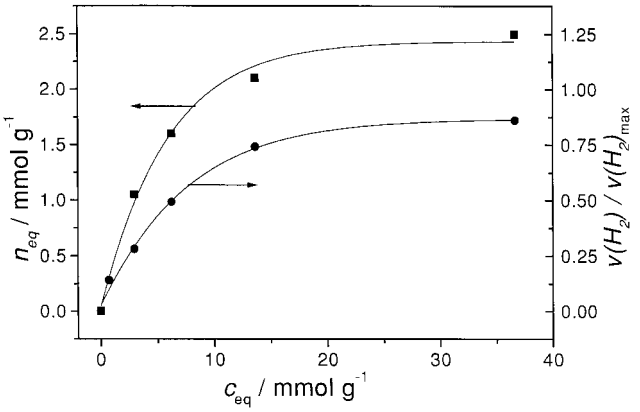

Figure 8. Dependence of amount of 2,5-DHF adsorbed (■) and initial rate (●) on equilibrium concentration of 2,5-DHF.

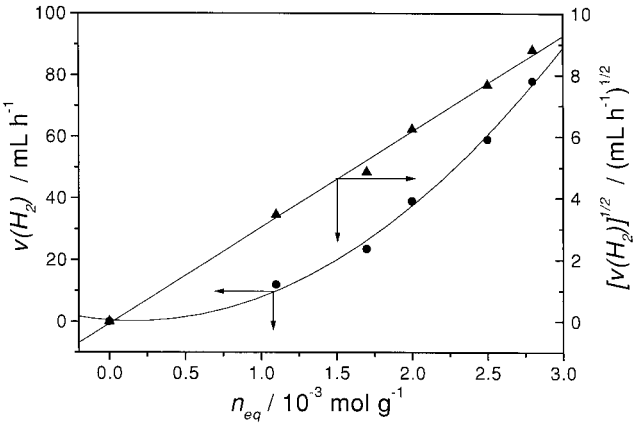

Figure 9. Dependence of rate of reaction (●) and its square root (▲) on the amount of 2,5-DHF adsorbed.

Evidence that dimerization of the radicals is a surface reaction is obtained from competition experiments with mixtures of 2,5-DHF and THF. Although 2,5-DHF reacts only ten times faster than THF, no THF dehydrodimers could be detected[8b] at a THF/2,5-DHF molar ratio of 10:1, irrespective of the catalyst concentration, but these products did appear when the ratio was increased to 580:1. In the presence of 0.5 and 1.5 g of ZnS-A, the percentage of bidihydrofuryls, mixed dehydrodimers, and 2,2′-bitetrahydrofuryl was 90, 9, and 1% and 82, 13, and 5%, respectively. In contrast, the corresponding composition was 5, 10, and 15% when the radicals were generated by photolysis of H_2O_2 in a mixture (15:1) of THF/2,5-DHF (the difference from 100% is balanced by hydroxylation products which are absent in the reaction catalyzed by zinc sulfide). This difference between the product ratio in the heterogeneous and homogeneous systems suggests that the radical C–C coupling occurs in the solvent–solute surface monolayer.

In contrast to the adsorption of imines to CdS,[7b] in the present case the true adsorption constant K_{ad} (170 ± 30 L mol^{-1}) is in fair agreement with the pseudo-constant (260 ± 50 L mol^{-1}) obtained from the concentration dependence of reaction rates by a modified Langmuir plot ($v(H_2)^{-1/2}$ against c_{eq}^{-1}, not shown). The average area of 10.2 Å^2 occupied by 2,5-DHF in the solvent–solute monolayer agrees

with the calculated value, $3.8\ \text{Å} \times 2.4\ \text{Å} = 9.1\ \text{Å}^2$, for an unsolvated molecule adsorbed edge-on to the surface. Within the limits of this adsorption model the average distance between the 2,5-DHF molecules is estimated as 4 Å. From the surface density of zinc sites ($11.4 \times 10^{-6}\ \text{mol m}^{-2}$ as reported for cubic ZnS[30]) and the specific surface area of ZnS-B_1 ($100-170\ \text{m}^2\,\text{g}^{-1}$) it is concluded that the surface concentration of 2,5-DHF in the saturated monolayer should be in the $(1-2) \times 10^{-3}\ \text{mol g}^{-1}$ range. This fits well with the experimentally observed value of $2.8 \times 10^{-3}\ \text{mol g}^{-1}$ and therefore suggests that 2,5-DHF is adsorbed onto zinc sites. This is corroborated by the ^{13}C NMR spectra of 2,5-DHF and other substrates adsorbed onto ZnS-B_1 from the gas phase, as described for ZnO[31] (although comparison of the latter results with the adsorption studies on aqueous suspensions is reliable only in some basic aspects).

Upon adsorption of cyclohexene and cyclopentene from the gas phase, all signals are shifted downfield ($\Delta\delta = 0.3$ and 0.8 compared with $CDCl_3$ and aqueous solution) (Table 2).[32] This suggests that adsorption, probably through π-complex formation at an electron-deficient surface center, is rather weak. In agreement with the more covalent character of ZnS, the adsorption shifts are smaller than reported for ZnO ($\Delta\delta = 2-4$).[31] For THF and 2,5-DHF the two α-carbon atoms appear as broad singlets shifted to lower field ($\Delta\delta = 0.7$ and 1.5, respectively), and indicate adsorption through the oxygen atom. In the case of 2,5-DHF the small downfield shift ($\Delta\delta = 0.4$) observed for the olefinic signals suggests that the C–C double bond is also involved, resulting in adsorption parallel to the zinc sulfide surface. This differs from adsorption from the aqueous solution where an orientation perpendicular to the surface (that is, without involvement of the double bond) is more likely (vide supra).

Table 2. ^{13}C NMR chemical shifts (δ) of various ethers and olefins in $CDCl_3$ solution and adsorbed onto ZnS-B_1.

Substrate	α-C (sp^3)		β-C (sp^3)		C (sp^2)	
	measured	ref. [32]	measured	ref. [32]	measured	ref. [32]
cyclohexene	26.0	25.4	23.3	23.0	127.9	127.4
cyclopentene	33.2	32.8	24.1	23.3	131.5	130.8
THF	69.1	68.4	26.6	26.5	–	–
2,5-DHF	76.9	75.4	–	–	126.8	126.4
2,3-DHF	69.5[a]	68.6[a]	–	–	145.6[c]	145.6[c]
	28.8[b]	28.5[b]	–	–	99.1[d]	98.4[d]
3,4-DHP	66.7[a]	64.9[a]	–	–	144.6[c]	145.6[c]
	23.5[b]	22.6[b]	19.7	19.3	100.7[d]	99.2[d]
dioxane	68.6	67.6	–	–	–	–

[a] -CH_2O-. b) =$CH(CH_2)$-. [c] =CHO-. [d] =$CH(CH_2)$-.

The enolic ethers 2,3-DHF and 3,4-DHP exhibit slightly different behavior. While the α-CH_2 signals ($\Delta\delta = 0.9$ for 2,3-DHF and 1.8 for 3,4-DHP) and olefinic β-carbon atoms ($\Delta\delta = 0.7$ for 2,3-DHF and 1.5 for 3,4-DHP) suffer deshielding, the signals of the olefinic α-carbon atoms are either not influenced or are shifted upfield ($\Delta\delta = 1.0$), respectively. These differences suggest that the enol ethers adsorb at a single zinc atom, whereas two zinc atoms are involved in the case of allyl ethers. A similar bridged surface complex seems to be formed with dioxane, which exhibits only one NMR signal shifted downfield ($\Delta\delta = 1.0$).

Mechanism of the oxidative step: The oxidation of 2,5-DHF to the corresponding allylic radical may proceed by two main reaction pathways, as discussed recently for the CdS-catalyzed photoaddition of 2,5-DHF to benzophenone imine:[3d] direct oxidation by the reactive hole coupled with a concerted or stepwise deprotonation (see Scheme 1) or indirect oxidation by H-atom abstraction from the cyclic ether by an oxidatively produced sulfur radical. Although such radicals have been observed on the surface of irradiated ZnS,[9, 33] the latter process is unlikely since THF is also reactive but in homogeneous solution does not undergo hydrogen abstraction by sulfur radicals such as MeS.[34] The concerted and stepwise oxidation mechanisms can be distinguished as follows. The actual potentials for THF and 2,5-DHF are easily determined (2.9, 2.3 V versus NHE, MeCN),[35a] but the reduction potential of the reactive hole can only be estimated from the position of the valence band edge of ZnS single crystals in contact with neutral water ($E_{vb} = 1.8$ V)[36d] and the observation that the flat-band potential of a semiconductor crystal may be shifted by about 0.4 V upon changing the nature of the adsorbed substrates.[36] Accordingly, for the ZnS powder employed in this study a range of 1.6–2.0 V seems reasonable. Thus, the electron transfer step of the stepwise mechanism is endergonic by at least 0.9 and 0.3 eV for the saturated and unsaturated ether, respectively. This makes the stepwise mechanism unlikely although the intermediate dihydrofuryl radical cation is a strong acid ($pK_a \approx -17$)[37, 38] and deprotonation of radical cations is a fast process with rate constants in the range $10^5-10^{10}\ \text{s}^{-1}$.[39] Further evidence against this mechanism stems from a plot of the apparent quantum yields[41] for the various ethers as a function of the calculated redox potentials (Figure 10).[35] Whereas the observed increase from THF to 3,6-dihydrodioxepine (3,6-DHD), 3-methyl-2,3-dihydropyran (3-MeDHP), and 2,5-DHF parallels the decrease in oxidation potential, the quantum yield decreases for the two enolic ethers 2,3-DHF and 3,4-DHP although they are much more easily oxidized than 2,5-DHF. This strong deviation suggests that the concerted mechanism (dissociative electron transfer) may be operating [Eq. (6)].

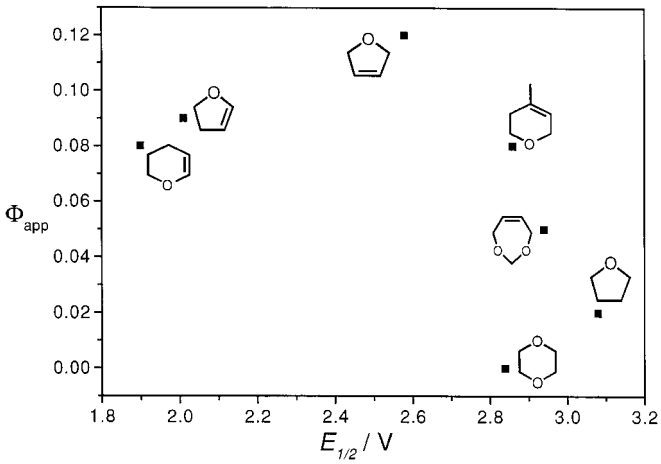

Figure 10. Dependence of apparent quantum yield ($\lambda_{exc} = 313$ nm) on substrate oxidation potential.

0947-6539/99/0501-0214 $ 17.50+.50/0 *Chem. Eur. J.* **1999**, *5*, No. 1

The driving force for this process corresponds to the difference between the free enthalpy of C–H bond homolysis and the potential of the hydrogen electrode [Eq. (6)].[40]

$$RH \rightarrow R^{\cdot} + H^{+} + e^{-} \quad (6)$$

An estimate for 2,5-DHF and THF reveals that, in contrast to the stepwise radical formation, the concerted pathway is exergonic by at least 0.9 and 0.2 eV, as indicated by the free enthalpy change of 0.72 and 1.38 eV, respectively.

Since no experimental data on bond dissociation energies (BDEs) are available, ab initio calculations were performed. The BDE is the difference between the sum of the total energies of the R$^{\cdot}$ and H$^{\cdot}$ radicals and the total energy of RH in its minimum-energy conformation. All molecules were fully optimized by DFT methods employing the Becke three-parameter hybrid (B3) exchange functional in combination with the Lee–Yang–Parr (LYP) correlation functional.[42] Contrary to the particularly poor predictions of the local spin density approximation (LSDA) methods, it has been shown that reliable bond dissociation energies (BDEs) are computed by B3LYP.[42] The calculated heats of formation of the compounds RH, their corresponding radicals, the BDEs, and stabilization energies of the radicals are shown in Table 3.

Table 3. Computed heats of formation (HF), zero-point energies (ZPE), stabilization energies (SE), and bond dissociation energies (BDE).

HF_{RH}	[au]	ZPE_{RH}[a]	$HF_{R^{\cdot}}$ [au]	ZPE_{R}[a]	SE[a]	BDE[a]
THF	–232.50339	73.24	–231.84701	64.76	–13.40	89.30
2,3-DHF	–231.27644	58.14	–230.63810	49.34	–25.04	77.67
2,5-DHF	–231.27042	57.91	–230.63810	49.34	–28.59	74.12
3,4-DHP	–270.60715	76.86	–269.96701	68.19	–23.79	78.91
3-MeDHP	–309.92669	94.04	–309.29467	85.58	–28.67	74.03
dioxane	–307.73269	76.81	–307.07096	68.12	–10.27	92.43
3,6-DHD	–345.82690	79.79	–345.19584	71.49	–29.12	73.58

[a] kcal mol^{-1}.

A plot of the quantum yield as a function of the BDE reveals a straight line for dioxane, THF, 3,4-DHP, 2,3-DHF, and 2,5-DHF (Figure 11). This clearly suggests that the quantum yield is governed by the dissociative electron transfer; that is, in the series of five-membered compounds the variation in BDE determines the quantum efficiency. The deviations observed for six-membered 3-MeDHP and 3,6-DHD may be due to steric hindrance of radical C–C coupling by the methyl group and to the presence of a second oxygen which renders the molecular structure too different from the other substrates.

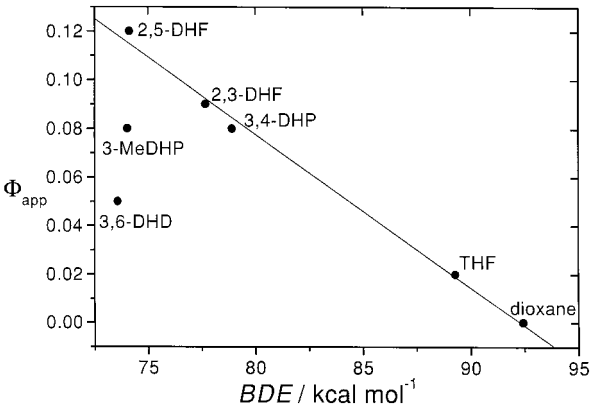

Figure 11. Dependence of apparent quantum yield on calculated bond dissociation energy (BDE).

Experimental Section

General methods: All experiments were performed under an argon atmosphere. 2,5-DHF was purified from furan by heating it with maleic acid anhydride for 3 h and subsequent distillation. All olefinic substrates were commercially available. For general procedures and apparatus see refs. [3b, 3d].

Instrumentation:

Static emission measurements: Perkin-Elmer LS 50B luminescence spectrometer, excitation and emission monochromator slits 5.0 nm, two scans with speeds of 240 nm min^{-1} at $\lambda_{exc} = 320$ nm.

Time-resolved emission measurements: Frequency-doubled synchronous pumped Rhodamine 6G dye laser ($\lambda = 306$ nm); luminescence curves were fitted to multiexponential decay according to Equation (7).

$$I(t) = I_1(t)\,e^{-t/\tau_1} + I_2(t)\,e^{-t/\tau_2} + ... + I_x(t)\,e^{-t/\tau x} \quad (7)$$

Apparent quantum yield: Mülheim -type electronic integrating actinometer,[8b] irradiation source Osram HBO 500 W, calibration with ferrioxalate, average of three experiments, experimental error less than ±10%; irradiation: Philips HPK 125 W high-pressure mercury lamp, unless otherwise stated (photon flux ≈ 10^{-4} Einstein s^{-1} (250 nm < λ < 400 nm)). ZnS-B_1 was used throughout all the experiments, unless noted otherwise. Hydrogen evolution was measured continuously with a volumetric device.[8] Initial rates were calculated from tangents to experimental hydrogen evolution curves at $t = 0$ (experimental error ±2%). It was ensured by appropriate control experiments that the rate of H_2 formation was equal to that of the dehydrodimers. All potentials $E_{1/2}$ are referred to an NHE and were calculated for acetonitrile solution from the following ionization potentials according to ref. [35a]: 9.14 (2,5-DHF[35b]), 8.50 (2,3-DHF[35b]), 9.70 (THF[35b]), 9.43 (dioxane[35b]), 9.02 (cyclopentene[35c]), 9.12 (cyclohexene[35c]), 8.37 (3,4-DHP[35d, 35e]), 9.45 (3-methyl-2,3-dihydropyran[35d, 35e]), 9.54 eV (3,6-dihydrodioxepine[35f]).

Preparation of ZnS samples:

ZnS-A: Under an argon atmosphere an aqueous solution (250 mL) of $Na_2S \cdot 9H_2O$ (24.0 g, 0.1 mol) was added dropwise to a solution of $ZnSO_4 \cdot 7H_2O$ (28.8 g, 0.1 mol) in water (250 mL). The mixture was stirred for 24 h and filtered, then the powder was washed with H_2O to neutrality and dried over Siccapent. The specific surface area determined by the BET method was 220 m^2 g^{-1}.

ZnS-A/S^{2-}, ZnS-A/Zn^{2+}: ZnS-A/S^{2-} and ZnS-A/Zn^{2+} were prepared in the presence of a 20% excess of $Na_2S \cdot 9H_2O$ (28.8 g, 0.12 mol) and of $ZnSO_4 \cdot 7H_2O$ (34.6 g, 0.12 mol), respectively.

ZnS-B_1, ZnS-B_2: A solution of NaOH (100.0 g, 2.5 mol) in H_2O (200 mL) was added to a solution of $ZnSO_4 \cdot 7H_2O$ (28.8 g, 0.1 mol) in H_2O (200 mL). After redissolution of $Zn(OH)_2$, thiourea (15.2 g, 0.2 mol) in H_2O (400 mL) was added. For ZnS-B_1 and ZnS-B_2 the mixture was heated to 80 °C for 48 h and 1 h, respectively, with occasional shaking. After filtration, the powder was washed and dried as described for ZnS-A. Specific surface areas of 170 (ZnS-B_1) and 37 m^2 g^{-1} (ZnS-B_2) were measured.

ZnS–Ventron: The commercially available ZnS–Ventron (99.99%) was used as obtained.

ZnS colloids: $Na_2S \cdot 9H_2O$ (0.48 g, 2.0 mmol), dissolved in water (20 mL), was added dropwise to a solution of $ZnSO_4 \cdot 7H_2O$ (0.58 g, 2.0 mmol) in water (20 mL)at 0 °C. Stirring was continued at this temperature for 10 min.[14]

Catalytic activity and corrosion behavior of ZnS samples: In a Pyrex immersion lamp apparatus ($\lambda \geq 290$ nm) the suspension of ZnS (0.1 g,

1.3 g L^{-1}) in water (70 mL) was sonicated for 20 min under a slow argon stream. After addition of 2,5-DHF (5 mL, 69 mmol), irradiation was conducted for 1 h.

For colloidal ZnS, the colloid solution (18 mL) was sonicated in a 20-mL cylindrical cuvette as described above and 2,5-DHF (1.2 mL, 18 mmol) was added before irradiation on an optical train (Osram HBO 500 W, $\lambda \geq 290$ nm).

The photostability of the various catalysts was tested in the absence of a sacrificial substrate. Formation of elemental zinc and cadmium was made evident by the appearance of the blue radical cation MV$^{\bullet+}$ upon addition of solid $(MV)Cl_2$. Elemental sulfur was detected as an anodic photocorrosion product by extraction of the reaction mixture with CS_2 and subsequent measurement of the absorbance at 350 nm.

ZnS emission and quenching: The corresponding ZnS sample (5 mg, 1.4 g L^{-1}) was suspended in H_2O (3.5 mL); for sulfide quenching Na_2S (0.16 mol g^{-1}) was used. The emission spectra of the aqueous ZnS suspensions were identical to those of the solid probes.[11] An apparent emission at 390 nm was identified as scattered light by comparison with an aqueous suspension of $BaSO_4$ exhibiting the same peak. At an excitation wavelength λ_{exc} of 320 nm a Raman scattering peak of H_2O was observed at 363 nm. For quenching experiments the ZnS samples were suspended in an aqueous quencher solution (3.5 mL) and sonicated under argon for 10 min before measurement. The concentrations of the metal sulfate solutions (Zn^{2+}, Cd^{2+}, Al^{3+}, Mg^{2+}) were 5.71×10^{-4} and 5.71×10^{-2} mol L^{-1}. Cd^{2+} induced a weak band at 520 nm in the excitation spectrum. The concentrations of the organic substrates 2,5-DHF and dioxane were 0.63 mol L^{-1}.

Inhibition experiments: For each experiment ZnS-B_1 (0.1 g, 1.3 g L^{-1}) was sonicated for 15 min under Ar in a metal sulfate or sodium sulfide solution (70 mL) of given concentration, then 2,5-DHF (5 mL, 69 mmol) was added. Irradiations were performed in a quartz immersion lamp apparatus ($\lambda >$ 254 nm). In all the experiments the concentration of 2,5-DHF was set at 0.9 mol L^{-1} (0.7 mol g^{-1}). The concentrations (c_s) were in the range 10^{-5}–10^{-1} and 10^{-6}–10^{-3} mol g^{-1} for Zn^{2+} and Cd^{2+}, respectively.

One reaction suspension, irradiated for 1 h under conditions of total inhibition of hydrogen evolution ($c_s(Cd^{2+}) = 7.8 \times 10^{-3}$ mol g^{-1}), was filtered, extracted with CCl_4, dried over $MgSO_4$, and analyzed by GC–MS to detect organic oxidation products.[8b]

To determine whether cadmium metal formation is due to excitation of ZnS or surface CdS, ZnS-B_1 was irradiated on an optical train equipped with an XBO 150 W lamp and a cut-off filter ($\lambda \geq 465$ nm, $c_s(Cd^{2+}) = 3.8 \times 10^{-3}$ mol g^{-1}, c_s(2,5-DHF) = 0.7 mol g^{-1}).

Dark adsorption experiments: Solute adsorption onto ZnS-B_1 (1.3 g L^{-1}) was followed by measuring the residual solute concentration after stirring aliquots (10 mL) of aqueous solutions with different initial concentrations for 20 h at room temperature in the dark (to prevent photoreactions, the glass tubes were completely wrapped with aluminum foil). After filtration (Millipore filter, pore size 0.2 μm), equilibrium concentrations of the metal ions and 2,5-DHF were measured by atomic absorption spectrometry (detection limit about 10^{-7} mol L^{-1}) and HPLC, respectively. The differences $\Delta c = c_{ini} - c_{eq}$ were normalized to n_{eq}, the number of moles of solute adsorbed per gram of ZnS. All values reported are the average of two measurements; observed deviations were less than ±5 %. The corresponding metal salt concentrations (c_s) were in the range 10^{-5}–10^{-3} and 10^{-7}–10^{-3} mol g^{-1} for Zn^{2+} and Cd^{2+}, respectively. The 2,5-DHF concentration was varied from 10^{-3} to 1.2 mol g^{-1}.

The HPLC calibration for aqueous 2,5-DHF solutions was performed three times at eight concentrations; deviation was ±2 %. The detector was not sufficiently sensitive to allow reliable measurements of THF adsorption.

Dependence of rate of H_2 evolution on the concentrations of 2,5-DHF and THF: ZnS-B_1 (0.1 g, 1.3 g L^{-1}) was suspended and sonicated for 15 min under argon in the corresponding substrate mixture (75 mL) (vide infra). Irradiation ($\lambda \geq 254$ nm) was performed for 1 h employing the immersion lamp apparatus mentioned above. 2,5-DHF and THF concentrations were varied from 10^{-3} to 1.2 mol g^{-1} and from 0.5 to 9.8 mol g^{-1}, respectively.

Competition experiments between 2,5-DHF and THF: In a Pyrex immersion lamp apparatus ($\lambda > 290$ nm), the suspension of ZnS-A (0.5 g, 2.3 g L^{-1} or 1.5 g, 6.9 g L^{-1}) in the substrate mixtures described below was sonicated for 10 min under an argon atmosphere and irradiated for 20 h. The products were obtained by extraction with diethyl ether, drying over $MgSO_4$, and careful removal of the solvent under reduced pressure (room temperature, 1 Torr), then identified by GC and GC–MS by co-injection of the authentic dehydrodimers, as described recently.[8b] [2,5-DHF]/[THF] = 1:580; 0.38 mL (5.0 mmol) of 2,5-DHF/210 mL (2.9 mol) of THF; 10 mL (0.6 mol) of H_2O.

Homogeneous photolysis experiments were performed by irradiating a mixture of H_2O_2 (8 mL, 0.3 mol), 2,5-DHF (6.7 mL, 89 mmol), and THF (100 mL, 1.4 mol) for 10 h in the apparatus described above.

^{13}C NMR spectra of substrates adsorbed onto ZnS-B_1: A dried NMR tube was filled with ZnS-B_1 (1 g) and evacuated several times, then adsorbate (THF, dioxane, 2,5-DHF, cyclopentene, cyclohexene, 3,4-DHP, or 2,3-DHF) was introduced in the vapor phase and the spectra were recorded at room temperature.[31] A susceptibility correction ($\Delta\delta = 1.2$) was applied to the chemical shifts, based on the upfield shift ($\Delta\delta = -1.2$) observed for TMS physisorbed onto ZnS-B_1.

Dependence of quantum yield on substrate structure: A stock solution was prepared from water (10 mL), dioxane (20 mL), and the corresponding substrate (27 mmol): 2,5-DHF (2.0 mL), 2,3-DHF (2.0 mL), 3,4-dihydro-2*H*-pyran (2.5 mL), 5,6-dihydro-4-methyl-2*H*-pyran (2.9 mL), cyclohexene (2.7 mL), dioxane (2.1 mL), THF (2.2 mL), or 2,5-dihydrodioxepine (2.6 mL), respectively. The stock solution (3 mL) was used to suspend ZnS-B_1 (5 mg, 1.7 g L^{-1}) in a 4-mL two-stopcock cuvette. After sonication for 10 min under a slow stream of nitrogen, the stirred suspension was irradiated on an optical train at $\lambda = 313$ nm (HBO 500W) for 0.5 h. The amount of hydrogen produced was measured by GC as described in detail in ref. [8b].

Acknowledgements

This work was supported by Volkswagen-Stiftung and Fonds der Chemischen Industrie. We also thank Prof. G. Emig for continuous support in specific surface area determinations and Prof. S. Schneider for assistance in the time-resolved measurements.

[1] a) P. V. Kamat, *Chem. Rev.* **1993**, *93*, 267; b) D. W. Bahnemann, M. Hilgendorff, R. Memming, *J. Phys. Chem. B*, **1997**, *101*, 4265.
[2] a) M. A. Fox, M. T. Dulay, *J. Photochem. Photobiol. A: Chem.* **1996**, *98*, 91; b) R. B. Draper, M. A. Fox, *Langmuir* **1990**, *6*, 1396; c) P. V. Kamat, *J. Phys. Chem.* **1989**, *93*, 859; d) D. P. Colombo, R. M. Bowman, *J. Phys. Chem.* **1996**, *100*, 16445.
[3] a) R. Künneth, Ch. Feldmer, H. Kisch, *Angew. Chem.* **1992**, *104*, 1102; *Angew. Chem. Int. Ed. Engl.* **1992**, *31*, 1039; b) R. Künneth, Ch. Feldmer, F. Knoch, H. Kisch, *Chem. Eur. J.* **1995**, *1*, 441; c) W. Schindler, F. Knoch, H. Kisch, *Chem. Ber.* **1996**, *129*, 925; d) H. Keck, W. Schindler, F. Knoch, H. Kisch, *Chem. Eur. J.* **1997**, *3*, 1638.
[4] S. Yanagida, H. Kawakami, K. Hashimoto, T. Sakata, C. Pac, H. Sakurai, *Chem. Lett.* **1984**, 1449.
[5] H. Al-Ekabi, P. de Mayo, *Tetrahedron* **1986**, *42*, 6277.
[6] C. S. Turchi, D. F. Ollis, *J. Catal.* **1990**, *122*, 178.
[7] a) J. Cunningham, S. Srijaranai, *J. Photochem. Photobiol. A: Chem.* **1991**, *58*, 361; b) W. Schindler, H. Kisch, *Photochem. Photobiol. A: Chem.* **1997**, *103*, 257.
[8] a) J. Bücheler, N. Zeug, H. Kisch, *Angew. Chem.* **1982**, *94*, 792; *Angew. Chem. Int. Ed. Engl.* **1982**, *21*, 783; b) N. Zeug, J. Bücheler, H. Kisch, *J. Am. Chem. Soc.* **1985**, *107*, 1459.
[9] Y. Nakaoka, Y. Nosaka, *Langmuir* **1997**, *13*, 708.
[10] S. Yanagida, H. Kawakami, Y. Midori, H. Kizumoto, C. Pac, Y. Wada, *Bull. Chem. Soc. Jpn.* **1995**, *68*, 1811.
[11] R. Künneth, G. Twardzik, G. Emig, H. Kisch, *J. Photochem. Photobiol. A: Chem.* **1993**, *76*, 209.
[12] The specific concentration c_s [mol g^{-1}] is normalized to the amount of ZnS present; the amount adsorbed at equilibrium is n_{eq} [mol g^{-1}].
[13] a) K. Sooklal, B. S. Cullum, S. M. Angel, C. J. Murphy, *J. Phys. Chem.* **1996**, *100*, 4551; b) L. Spanhel, M. Haase, H. Weller, A. Henglein, *J. Am. Chem. Soc.* **1987**, *109*, 5649; c) A. Henglein, *Ber. Bunsenges. Phys. Chem.* **1982**, *86*, 301.
[14] S. Yanagida, Y. Ishimura, Y. Myake, T. Shiragami, C. Pak, K. Hashimoto, T. Sakata, *J. Phys. Chem.* **1989**, *93*, 2576.

  0947-6539/99/0501-0216 $ 17.50+.50/0 *Chem. Eur. J.* **1999**, *5*, No. 1

[15] a) S. Yanagida, Y. Ishimura, Y. Miyake, T. Shiragami, C. Pak, K. Hashimoto, T. Sakata, *J. Phys. Chem.* **1992**, *96*, 3521; b) A. Henglein, *Top. Curr. Chem.* **1988**, *1988*, 113.
[16] S. Yanagida, H. Kawakami, K. Hashimoto, T. Sakata, C. Pac, H. Sakurai, *Chem. Lett.* **1984**, 1449.
[17] a) W. J. Albery, P. N. Bartlett, C. P. Wilde, J. D. Darwent, *J. Am. Chem. Soc.* **1985**, *107*, 1854; b) W. J. Albery, G. T. Brown, J. R. Darwent, E. Saievar-Iranizad, *J. Chem. Soc. Faraday Trans. 1* **1985**, *81*, 1999; c) D. R. James, Y.-S. Liu, P. de Mayo, W. R. Ware, *Chem. Phys. Lett.* **1985**, *120*, 460.
[18] For starting concentrations higher than 1.5 mmol g^{-1} the experimental error increased to $\pm 25\%$, because of the high dilution factor. These results therefore represent only qualitative trends.
[19] J. Cunningham, P. Sedlak, *J. Photochem. Photobiol. A: Chem.* **1994**, *77*, 255.
[20] G. Hörner, H. Kisch, unpublished results.
[21] J. S. Clunie, B. T. Ingram, *Adsorption from Solution at the Solid/Liquid Interface* (Eds.: G. D. Parfitt, C. H. Rochester), Academic Press, London, **1983**, chapter 4.
[22] a) A. W. Adamson, *Physical Chemistry of Surfaces,* 4th ed., Wiley, New York, **1982**; b) P. C. Hiemenz, *Principles of Colloid and Surface Chemistry,* 2nd ed., Marcel Dekker, New York, **1986**.
[23] S. W. Park, C. P. Huang, *J. Colloid Interface Sci.* **1989**, *128*, 245.
[24] L. Zang, C.-Y. Liu, X.-M. Ren, *J. Photochem. Photobiol. A: Chem.* **1994**, *79*, 197.
[25] H. Weller, U. Koch, M. Gutierrez, A. Henglein, *Ber. Bunsenges. Phys. Chem.* **1984**, *88*, 649.
[26] a) G. H. Aylward, T. J. V. Findlay, *Datensammlung Chemie in SI-Einheiten,* 2nd ed., Verlag Chemie, Weinheim, **1981**; b) the effect of adsorption on the redox potential of the metal ions is neglected.
[27] From the adsorption constant of zinc ions, $K = 2.0$,[20] a value of about 1.7 kJ mol^{-1} is obtained for the free adsorption enthalpy. According to a rule of thumb (J. M. Thomas, W. J. Thomas, *Principles And Practice Of Heterogeneous Catalysis*, VCH, Weinheim, **1997**, p. 119) the activation energy of surface diffusion should be in the range of only 0.17 – 0.34 kJ mol^{-1} (that is, 10 – 20 % of ΔG_{ad}), allowing application of the Stern – Volmer model.
[28] Although the lifetime of the reactive electron – hole pair is not known, the reasonable estimate of 10^{-6} – 10^{-9} s leads to an electron transfer rate constant between 10^{10} and 10^{13} L mol^{-1} s^{-1}. In general, electron transfer reactions at the semiconductor – liquid interface are very fast (see ref. [1] and *Homogeneous and Heterogeneous Photocatalysis* (Eds.: N. Serpone, E. Pelizzetti), D. Reidel, Dordrecht, **1986**, p. 51).
[29] F. Wilkinson, *Chemical Kinetics and Reaction Mechanisms*, Van Nostrand Reinhold, Wokingham (UK), **1980**.
[30] Q. Zhang, Z. Xu, J. A. Finch, *J. Colloid Interface Sci.* **1995**, *169*, 414.
[31] I. T. Ali, I. D. Gay, *J. Phys. Chem.* **1981**, *85*, 1251.
[32] H. O. Kalinowski, S. Berger, S. Braun, *^{13}C-NMR-Spektroskopie*, Thieme, Stuttgart, **1984**.
[33] a) M. Anpo, A. Matsumoto, S. Kodama, *J. Chem. Soc. Chem. Commun.* **1987**, 1038; b) S. Kodama, A. Matsumoto, Y. Kubokawa, M. Anpo, *Bull. Chem. Soc. Jpn.* **1986**, *59*, 3765; c) S. Yanagida, K. Mizumoto, C. Pak, *J. Am. Chem. Soc.* **1986**, *108*, 647.
[34] L. Lunazzi, G. Placucci, L. Grossi, *Tetrahedron* **1983**, *39*, 159.
[35] a) $E_{1/2}$ is estimated from the ionization potential (IP [eV]; see Experimental Section) according to the relation $E_{1/2} = 0.89 \times \mathrm{IP} - 6.04 + 0.49$; the actual potential was obtained by applying the Nernst equation, taking concentrations of 10^{-6} and 10^{-1} mol L^{-1} for the 2,5-DHF radical cation and 2,5-DHF, respectively (L. Miller, G. D. Nordblom, E. A. Mayeda, *J. Org. Chem.* **1972**, *37*, 916); b) see reference 41 in ref. [8b]; c) E. Heilbronner, *Helv. Chim. Acta* **1970**, *53*, 1677; d) M. Bloch, F. Broglie, E. Heilbronner, T. B. Jones, H. Prinzbach, O. Schweikert, *Helv. Chim. Acta* **1978**, *61*, 1388; e) D. A. Demeo, M. A. El-Sayed, *J. Chem. Phys.* **1970**, *52*, 2622; f) V. V. Zverev, J. Villem, E. N. Klimovitskii, B. A. Arbuzov, *Zh. Obshch. Khim.* **1982**, *52(8)*, 1888.
[36] a) M. Bruening, E. Moons, D. Yaron-Marcovich, D. Cahen, J. Libman, A. Shanzer, *J. Am. Chem. Soc.* **1994**, *116*, 2972; b) M. Bruening, E. Moons, D. Cahen, A. Shanzer, *J. Phys. Chem.* **1995**, *99*, 8368; c) M. Bruening, R. Cohen, J. F. Guillemoles, T. Moav, J. Libman, A. Shanzer, D. Cahen, *J. Am. Chem. Soc.* **1997**, *119*, 5720; d) F.-R. Fan, P. Leempoel, A. J. Bard, *J. Electrochem. Soc.* **1983**, *130*, 1866.
[37] a) A. Albini, E. Fasani, N. d'Alessandro, *Coord. Chem. Rev.* **1993**, *125*, 269; b) A. M. De P. Nicholas, D. R. Arnold, *Can. J. Chem.* **1982**, *60*, 2165; c) J. P. Dinnocenzo, T. E. Banach, *J. Am. Chem. Soc.* **1989**, *111*, 8646; d) for pK_a calculations, $E_{1/2}$(2,5-DHF) = 2.6 V and BDE(2,5-DHF) = 74.12 kcal mol^{-1} (see Table 3).
[38] J. Fossey, D. Lefort, J. Sorba, *Free Radicals In Organic Chemistry*, Wiley, New York, **1995**.
[39] A. Anne, P. Hapiot, P. Neta, J.-M. Savèant, *J. Am. Chem. Soc.* **1992**, *114*, 4694.
[40] a) Calculated by using $E_0(H^+/H) = -2.40$ V(H_2O)[40b] and the BDE values given in Table 2; these were converted to the $\Delta G(H_2O)$ values by subtracting 0.1 eV for the solvent contribution.[40b] The same argument was used to explain the photooxidation of alcohols by ZnS;[40c] b) V. D. Parker, *J. Am. Chem. Soc.* **1992**, *114*, 7458; c) A. Henglein, M. Gutierrez, Ch.-H. Fischer, *Ber. Bunsenges. Phys. Chem.* **1984**, *88,* 170.
[41] For problems of measuring quantum yields in heterogeneous systems, see: a) N. Serpone, *EPA Newslett.* **1997**, 35; b) C. A. Martin, M. A. Baltanas, A. E. Cassano, *J. Photochem. Photobiol. A: Chem.* **1996**, *94*, 173.
[42] M. J. Frisch, G. W. Trucks, H. B. Schlegel, P. M. W. Gill, B. G. Johnson, M. A. Robb, J. R. Cheeseman, T. Keith, G. A. Petersson, J. A. Montgomery, K. Raghavachari, M. A. Al-Laham, V. G. Zakrzewski, J. V. Ortiz, J. B. Foresman, C. Y. Peng, P. Y. Alaya, W. Chen, M. W. Wong, J. L. Andres, E. S. Replogle, R. Gomperts, R. L. Martin, D. J. Fox, J. S. Binkley, D. J. Defrees, J. Baker, J. P. Stewart, M. Head-Gordon, C. Gonzalez, J. A. Pople, *Gaussian-94,* Gaussian, Inc., Pittsburgh, PA, **1995**.
[43] a) B. G. Johnson, P. M. W. Gill, J. A. Pople, *J. Chem. Phys.* **1993**, *98*, 5612; b) A. St.-Amant in *Reviews in Computational Chemistry, vol. 7* (Eds.: K. B. Lipkowitz, D. B. Boyd), VCH, New York, **1996**, p. 21.

Received: February 11, 1998
Revised version: August 5, 1998 [F 1002]